Controlling and Fine Tuning the Physical Properties of Two Identical Metal Coordination Sites in De Novo Designed Three Stranded Coiled Coil Peptides

Olga Iranzo,[†,‡,ll] Saumen Chakraborty,[†,ll] Lars Hemmingsen,[§] and Vincent L. Pecoraro*,[†]

Department of Chemistry, University of Michigan, Ann Arbor, Michigan 48109, United States; Instituto de Tecnologia Química e Biológica, Universidade Nova de Lisboa, 2781-901 Oeiras, Portugal; and Department of Basic Sciences and Environment, University of Copenhagen, Thorvaldsensvej 40, 1871 Frederiksberg, Denmark

Received June 1, 2010; E-mail: vlpec@umich.edu

Abstract: Herein we report how de novo designed peptides can be used to investigate whether the position of a metal site along a linear sequence that folds into a three-stranded α-helical coiled coil defines the physical properties of Cd(II) ions in either CdS_3 or CdS_3O (O-being an exogenous water molecule) coordination environments. Peptides are presented that bind Cd(II) into two identical coordination sites that are located at different topological positions at the interior of these constructs. The peptide **GRAND**L16PenL19IL23PenL26I binds two Cd(II) as trigonal planar 3-coordinate CdS_3 structures whereas **GRAND**L12AL16CL26AL30C sequesters two Cd(II) as pseudotetrahedral 4-coordinate CdS_3O structures. We demonstrate how for the first peptide, having a more rigid structure, the location of the identical binding sites along the linear sequence does not affect the physical properties of the two bound Cd(II). However, the sites are not completely independent as Cd(II) bound to one of the sites (^{113}Cd NMR chemical shift of 681 ppm) is perturbed by the metalation state (apo or $[Cd(pep)(Hpep)_2]^+$ or $[Cd(pep)_3]^-$) of the second center (^{113}Cd NMR chemical shift of 686 ppm). **GRAND**L12AL16CL26AL30C shows a completely different behavior. The physical properties of the two bound Cd(II) ions indeed depend on the position of the metal center, having pK_{a2} values for the equilibrium $[Cd(pep)(Hpep)_2]^+ \rightarrow [Cd(pep)_3]^- + 2H^+$ (corresponding to deprotonation and coordination of cysteine thiols) that range from 9.9 to 13.9. In addition, the L26AL30C site shows dynamic behavior, which is not observed for the L12AL16C site. These results indicate that for these systems one cannot simply assign a "4-coordinate structure" and assume certain physical properties for that site since important factors such as packing of the adjacent Leu, size of the intended cavity (endo vs exo) and location of the metal site play crucial roles in determining the final properties of the bound Cd(II).

1. Introduction

Over the last two decades, the emerging field of de novo metalloprotein design has empowered chemists to understand biologically relevant metal binding sites at a molecular level and gain important fundamental knowledge on how the protein matrix influences and controls the metal ion properties.[1−3] Owing to significant advances in peptide synthesis and computational and structural biology, it has become possible to design linear amino acid sequences that generate scaffolds with a well-defined secondary and tertiary structure. This approach allows one to elucidate, in a systematic manner, structural features and elements that play crucial roles in determining the coordination geometries and physical properties of metal ions, as well as their site specificity. This degree of knowledge is necessary not only to comprehend fully how metalloproteins work and fine-tune the metal ion geometries and properties, but also for the design of new biomolecules with improved properties and new functionalities. Given this promise, it is not surprising that this research field is attracting a significant amount of attention as is shown by the reviews that have recently appeared.[4]

One of the most targeted secondary structural motifs in the de novo peptide design field is the α-helix and in general it has been used to generate α-helical coiled coils and bundle structures. These helical aggregates result from sequences containing a seven-residue [heptad] repeat, denoted [**abcdefg**]$_n$, that typically has hydrophobic residues at **a** and **d** positions, and polar or charged residues at **e** and **g** positions. Despite this

† Department of Chemistry, University of Michigan.
‡ Instituto de Tecnologia Química e Biológica, Universidade Nova de Lisboa.
§ Department of Basic Sciences and Environment, University of Copenhagen.
ll These authors contributed equally.

(1) DeGrado, W. F.; Summa, C. M.; Pavone, V.; Nastri, F.; Lombardi, A. *Annu. Rev. Biochem.* **1999**, *68*, 779–819.
(2) Gibney, B.; Rabanal, F.; Dutton, P. *Curr. Opin. Chem. Biol.* **1997**, *1*, 537–542.
(3) Peacock, A. F. A.; Iranzo, O.; Pecoraro, V. L. *Dalton Trans.* **2009**, 2271–2280.
(4) Lu, Y.; Yeung, N.; Sieracki, N.; Marshall, N. M. *Nature* **2009**, *460*, 855–862.

apparently simple pattern, the heptad repeat approach has shown its high versatility and potential. A wide variety of de novo designed structures have already been reported which differ in the nature (homomers/heteromers), number (from dimers to heptamers) and alignment (parallel/antiparallel) of the helices.[5] From an inorganic chemical point of view, these structures represent perfect scaffolds where diverse metal ion binding sites can be engineered. Indeed, this strategy has been employed by several research groups to design metallopeptides with specified characteristics.

Two major strategies have been employed to introduce metal ion binding sites into these helical scaffolds: (a) the use of cofactors, mainly heme units, or (b) the replacement of the amino acids in the hydrophobic cores by amino acids with metal ion coordinating properties. The Dutton and Gibney groups have used four-helix bundles as maquettes to study heme containing proteins.[6−9] Gibney and co-workers also used the maquette motifs to develop a prototype ferredoxin maquette, a peptide-based synthetic analogue of natural [4Fe-4S]$^{2+/+}$ proteins.[10] DeGrado,[11,12] Ghirlanda,[13] Lombardi and Pavone,[14] Mihara,[15,16] and their co-workers also used this approach to prepare different coiled coils and helical bundles which can bind between one and four heme units depending on the design. The second strategy was used by DeGrado and co-workers to design the dueferri (DF) peptides, a family of four-helix bundles, that contain a Glu$_4$-His$_2$ metal binding site capable of coordinating 2 equiv of Fe(II), Mn(II) and Zn(II). These de novo designed metallopeptides are paradigms for di-iron, dimanganese, and dizinc proteins.[17,18] The Ogawa group has designed Cys containing peptides which assemble into coiled coils upon binding Cd(II) and Cu(I), forming a CdS$_4$ and a Cu$_4$S$_4$ center, respectively.[19,20] On the same line, using Cys or His as donor ligands, Tanaka and co-workers designed peptides that bound Hg(II) and Cd(II),[21] and Ni(II), Zn(II), Co(II), and Cu(II),[22−24]

respectively. These last systems[19−23] and others[25,26] displayed metal-ion induced self-assembly.

Before one can use de novo design for the more lofty goal of chemical catalysis it is important to understand how to control the coordination environment of what would be the resting state of the active site. To this end, our group has used the de novo design approach to define the chemistry of Cd(II), Hg(II), As(III), and Pb(II) in thiolate rich environments, with particular emphasis on controlling the coordination number of the bound ions. Using the heptad repeat approach, we have described how (above pH 5.5) the parent peptide **TRI** (Table 1)[27] associates in aqueous solution to form parallel, three-stranded coiled coils. These aggregates bind metals in a sulfur rich environment ranging from HgS$_2$ (linear), HgS$_3$ (trigonal planar), and HgS$_4$ (tetrahedral) to As(III)S$_3$ (trigonal pyramidal).[28−31] We have also prepared peptides that contain either Cys or the noncoded amino acid analogue Pen (penicillamine) in their interiors, binding Cd(II) with high affinity and different coordination geometries. Substitution of the Leu by Cys or Pen generates partially or fully preorganized homoleptic thiol-rich binding sites inside the hydrophobic core of these coiled coils. By combining ^{113}Cd NMR and ^{111m}Cd Perturbed Angular Correlation (PAC) spectroscopies, we have shown how the peptide **TRI**L16C binds Cd(II) as a mixture of pseudotetrahedral (CdS$_3$O) and trigonal planar (CdS$_3$) structures.[32] Complete control of the Cd(II) coordination number was achieved by modifying the sterics in the metal ion binding site through changes in the amino acids of either the first or second coordination sphere. Namely, removal of steric bulk directly above the Cys plane by replacement of a Leu with an Ala generated the peptide **TRI**L12AL16C that binds Cd(II) exclusively in the CdS$_3$O geometry.[33,34] However, the pure CdS$_3$ geometry was achieved by increasing steric constrains around the metal ion binding site. Two different approaches were used in the latter case, both employing non-natural amino acids, a key benefit of the chemical peptide synthesis. In the first approach, Cys was replaced by Pen which has bulky methyl groups replacing the β-methylene hydrogen atoms (peptide **TRI**L16Pen).[34] In the second strategy, the chirality of the Leu just above the Cys was modified (L-Leu was replaced by D-Leu) and as a

(5) Iranzo, O.; Ghosh, D.; Pecoraro, V. L. *Inorg. Chem.* **2006**, *45*, 9959–9973.

(6) Gibney, B. R.; Rabanal, F.; Skalicky, J. J.; Wand, A. J.; Dutton, P. L. *J. Am. Chem. Soc.* **1999**, *121*, 4952–4960.

(7) Gibney, B. R.; Dutton, P. L. *Adv. Inorg. Chem.* **2001**, *51*, 409–455.

(8) Reedy, C. J.; Gibney, B. R. *Chem. Rev.* **2004**, *104*, 617–649.

(9) Zhuang, J.; Amoroso, J. H.; Kinloch, R.; Dawson, J. H.; Baldwin, M. J.; Gibney, B. R. *Inorg. Chem.* **2004**, *43*, 8218–8220.

(10) Kennedy, M. L.; Petros, A. K.; Gibney, B. R. *J. Inorg. Biochem.* **2004**, *98*, 727–732.

(11) Cochran, F. V.; Wu, S. P.; Wang, W.; Nanda, V.; Saven, J. G.; Therien, M. J.; DeGrado, W. F. *J. Am. Chem. Soc.* **2005**, *128*, 663.

(12) McAllister, K. A.; Zou, H.; Cochran, F. V.; Bender, G. M.; Senes, A.; Fry, H. C.; Nanda, V.; Keenan, P. A.; Lear, J. D.; Saven, J. G.; Therien, M. J.; Blasie, J. K.; DeGrado, W. F. *J. Am. Chem. Soc.* **2008**, *130*, 11921–11927.

(13) Ghirlanda, G.; Osyczka, A.; Liu, W.; Antolovich, M.; Smith, K. M.; Dutton, P. L.; Wand, A. J.; DeGrado, W. F. *J. Am. Chem. Soc.* **2004**, *126*, 8141–8147.

(14) Nastri, F.; Lombardi, A.; D'Andrea, L. D.; Sanseverino, M.; Maglio, O.; Pavone, V. *Peptide Sci.* **1998**, *47*, 5–22.

(15) Sakamoto, S. O., I.; Ueno, A.; Mihara, H. *J. Chem. Soc., Perkin Trans. 2,* **1999**, 2059–2069.

(16) Obataya, I.; Kotaki, T.; Sakamoto, S.; Ueno, A.; Mihara, H. *Bioorg. Med. Chem. Lett.* **2000**, *10*, 2719–2722.

(17) Calhoun, J. R.; Nastri, F.; Maglio, O.; Pavone, V.; A.;, L.; DeGrado, W. F. *Peptide Sci.* **2005**, *80*, 264–278.

(18) Geremia, S.; DiCostanzo, L.; Randaccio, L.; Engel, D. E.; Lombardi, A.; Nastri, F.; DeGrado, W. F. *J. Am. Chem. Soc.* **2005**, *127*, 17266–17276.

(19) Kharenko, O. A.; Ogawa, M. Y. *J. Inorg. Biochem.* **2004**, *98*, 1971–1974.

(20) Kharenko, O. A.; Kennedy, D. C.; Demeler, B.; Maroney, M. J.; Ogawa, M. Y. *J. Am. Chem. Soc.* **2005**, *127*, 7678–7679.

(21) Li, X. Q.; Suzuki, K.; Kanaori, K.; Tajima, K.; Kashiwada, A.; Hiroaki, H.; Kohda, D.; Tanaka, T. *Protein Sci.* **2000**, *9*, 1327–1333.

(22) Suzuki, K.; Hiroaki, H.; Kohda, D.; Nakamura, H.; Tanaka, T. *J. Am. Chem. Soc.* **1998**, *120*, 13008–13015.

(23) Kiyokawa, T.; Kanaori, K.; Tajima, K.; Koike, M.; Mizuno, T.; Oku, J.; Tanaka, T. *J. Peptide Res.* **2004**, *63*, 347–353.

(24) Shiga, D.; Nakane, D.; Inomata, T.; Masuda, H.; Oda, M.; Noda, M.; Uchiyama, S.; Fukui, K.; Takano, Y.; Nakamura, H.; Mizuno, T.; Tanaka, T. *Biopolymers* **2009**, *91*, 907–916.

(25) Ghosh, D.; Pecoraro, V. L. *Inorg. Chem.* **2004**, *43*, 7902–7915.

(26) Farrer, B.; Pecoraro, V. L. *Proc. Natl. Acad. Sci., U.S.A.* **2003**, *100*, 3760–3765.

(27) Dieckmann, G. R.; McRorie, D. K.; Lear, J. D.; Sharp, K. A.; DeGrado, W. F.; Pecoraro, V. L. *J. Mol. Biol.* **1998**, *280*, 897–912.

(28) Dieckmann, G. R.; McRorie, D. K.; Tierney, D. L.; Utschig, L. M.; Singer, C. P.; O'Halloran, T. V.; Penner-Hahn, J. E.; DeGrado, W. F.; Pecoraro, V. L. *J. Am. Chem. Soc.* **1997**, *119*, 6195–6196.

(29) Farrer, B. T.; Harris, N. P.; Balchus, K. E.; Pecoraro, V. L. *Biochemistry* **2001**, *40*, 14696–14705.

(30) Touw, D. S.; Nordman, C. E.; Stuckey, J. A.; Pecoraro, V. L. *Proc. Natl. Acad. Sci., U.S.A.* **2007**, *104*, 11969–11974.

(31) Luczkowski, M.; Stachura, M.; Schirf, V.; Demeler, B.; Hemmingsen, L.; Pecoraro, V. L. *Inorg. Chem.* **2008**, *47*, 10875–10888.

(32) Matzapetakis, M.; Farrer, B. T.; Weng, T.-C.; Hemmingsen, L.; Penner-Hahn, J. E.; Pecoraro, V. L. *J. Am. Chem. Soc.* **2002**, *124*, 8042–8054.

(33) Lee, K. H.; Matzapetakis, M.; Mitra, S.; Marsh, E. N. G.; Pecoraro, V. L. *J. Am. Chem. Soc.* **2004**, *126*, 9178–9190.

(34) Lee, K.-H.; Cabello, C.; Hemmingsen, L.; Marsh, E. N. G.; Pecoraro, V. L. *Angew. Chem., Int. Ed.* **2006**, *45*, 2864–2868.

Table 1. List of Different Derivatives of the **TRI** and **GRAND** Peptides

Peptide	Sequence
TRI	Ac-G LKALEEK LKALEEK LKALEEK LKALEEK G-NH$_2$
GRAND	Ac-G LKALEEK LKALEEK LKALEEK LKALEEK LKALEEK G-NH$_2$
TRIL12AL16C	Ac-G LKALEEK LKA**A**EEK **C**KALEEK LKALEEK G-NH$_2$
TRIL16Pen	Ac-G LKALEEK LKALEEK **X**KALEEK LKALEEK G-NH$_2$
GRANDL12AL16C	Ac-G LKALEEK LKA**A**EEK **C**KALEEK LKALEEK LKALEEK G-NH$_2$
GRANDL26AL30C	Ac-G LKALEEK LKALEEK LKALEEK LKA**A**EEK **C**KALEEK G-NH$_2$
GRANDL16Pen	Ac-G LKALEEK LKALEEK **X**KALEEK LKALEEK LKALEEK G-NH$_2$
GRANDL16PenL26AL30C	Ac-G LKALEEK LKALEEK **X**KALEEK LKA**A**EEK **C**KALEEK G-NH$_2$
GRANDL12AL16CL26AL30C	Ac-G LKALEEK LKA**A**EEK **C**KALEEK LK**A**LEEK **C**KALEEK G-NH$_2$
GRANDL12AL16CL26AL30CL33I	Ac-G LKALEEK LKA**A**EEK **C**KALEEK LK**A**LEEK **C**KA**I**EEK G-NH$_2$
GRANDL16PenL23PenL26I	Ac-G LKALEEK LKALEEK **X**KALEEK **X**KA**I**EEK LKALEEK G-NH$_2$
GRANDL16PenL19IL23PenL26I	Ac-G LKALEEK LKALEEK **X**KA**I**EEK **X**KA**I**EEK LKALEEK G-NH$_2$

X = Penicillamine. Residues in red indicate modifications.

consequence, the side chain of the Leu was reoriented toward the C-termini and toward the metal ion binding site (peptide **TRI**L12L$_D$L16C).[35] This knowledge has driven our design strategy for the heterochromic peptides, **GRAND**L16PenL-26AL30C and **GRAND**L12L$_D$L16CL26AL30C.[35,36] These peptides, containing two binding sites in close proximity (~20 Å) within the same three-stranded coiled coil, are capable of binding two Cd(II) ions with different coordination geometries (3-coordinate, trigonal planar as CdS$_3$ and 4-coordinate, pseudotetrahedral as CdS$_3$O) and thus different physical properties. Furthermore, these peptides show site-selective Cd(II) recognition, where in both peptides, Cd(II) binds selectively to the 4-coordinate site (CdS$_3$O) regardless of the pH conditions. These heterochromic peptides are important achievements toward our goal of preparing designed metalloproteins which contain both structural and catalytic sites.

While heterochromic peptides allowed us to discriminate between 3- and 4-coordination sites that were at a first glance nearly identical, this success raised an important new question: Are all 3-coordinate or 4-coordinate sites in the same peptide identical? Said differently, can we refer to, as an example, an environment simply as a 4-coordinate site or must we specify whether this sulfur rich environment is in the center of the helix versus an end or whether the Cys resides in **a** vs **d** heptad positions? And, if there is a difference, will the physical properties of the center be modified, the selectivity for binding sites or the dynamics of the structures be different? Ultimately, we can address whether the position of these sites in the coiled coil play any role in fine-tuning the physical properties of the bound Cd(II).

To address these issues we have designed sets of single peptides capable of binding 2 equiv of Cd(II) with the same coordination geometry. A construct such as this will have two 3-coordinate sites (CdS$_3$) or two 4-coordinate sites (CdS$_3$O) at

different positions in the coiled coil. Figure S1 of the Supporting Information, SI, shows models for these two constructs created in PyMol.[37] These peptides would allow us to directly assess the selectivity of metal binding between two equivalent positions within the peptide, whether binding of one metal would influence the physical properties of the second bound metal and if different physical properties can be observed for the same metal in two similar first coordination environments but in different topological positions within the coiled coil. With the constructs described herein, we address the important issues of how the specific position of these sites could modify the intrinsic properties of the bound Cd(II). We conclude that the 4-coordinate site is more sensitive to these changes than the 3-coordinate site, and discuss how the final physical properties of the 4-coordinate site can be modified by the intrinsic nature of the local peptide environment.

2. Experimental Section

The nomenclature used to describe the metal complexes prepared in this study is provided in ref 38.

2.1. Peptide Synthesis and Purification. The **TRI** and **GRAND** peptides (see Table 1 for sequence nomenclature) were synthesized on an Applied Biosystems 433A peptide synthesizer using standard Fmoc protocols,[39] and purified and characterized as described previously.[29]

2.2. Ultraviolet−Visible (UV−vis) Spectroscopy. All solutions were purged with argon before use to minimize the chances of oxidation of the peptides and formation of disulfide bonds. Fresh stock solutions of the purified peptides were prepared for each experiment in doubly distilled water and their concentrations determined by quantization of the Cys thiol groups using a known assay with 4,4′-dipyridyl disulfide.[40]

2.2.1. Metal Binding Titrations. Cd(II) into peptide titrations were performed at room temperature on a Cary 100 Bio UV−vis spectrometer using a 1-cm quartz cuvette. Aliquots of 8.93 mM CdCl$_2$ stock solution were added into a 3-mL solution containing 60 μM peptide and 50 mM appropriate buffer (TRIS for pH 8.5

(35) Peacock, A. F. A.; Hemmingsen, L.; Pecoraro, V. L. *Proc. Natl. Acad. Sci., U.S.A.* **2008**, *105*, 16566–16571.

(36) Iranzo, O.; Cabello, C.; Pecoraro, V. L. *Angew. Chem., Int. Ed.* **2007**, *46*, 6688–6691.

(37) DeLano, W. L. *The PyMOL Molecular Graphics System, DeLano Scientific*, Palo Alto, California, USA, 2005, http://www.pymol.org.

Table 2. Apparent pK_{a2} Values for **TRI** and **GRAND** Peptides

peptide	apparent pK_{a2}
TRIL12AL16C	12.2 ± 0.2
TRIL16Pen	15.8 ± 0.2
GRANDL12AL16C	11.3 ± 0.2
GRANDL26AL30C	9.9 ± 0.2
GRANDL16Pen	15.7 ± 0.2
GRANDL16PenL26AL30C	9.6 ± 0.2 (L26AL30C site)
	16.1 ± 0.2 (L16Pen site)
GRANDL12AL16CL26AL30C	11.8 ± 0.2 (L12AL16C site)
	13.9 ± 0.2 (L26AL30C site)
GrandL12AL16CL26AL30CL33I	11.6 ± 0.2 (L12AL16C site)
	13.5 ± 0.2 (L26AL30C site)
GRANDL16PenL19IL23PenL26I	15.2 ± 0.2 (L23Pen site)
	15.9 ± 0.2 (L16Pen site)

and CHES for pH 9.0 and 9.5). In each case, the difference spectra were obtained by subtracting the background spectrum of the peptide in the absence of metal (60 μM peptide and 50 mM appropriate buffer).

2.2.2. pH Titrations. UV−vis pH titrations were carried out at room temperature on an Ocean Optics SD 2000 fiber optic spectrometer and the pH measured using a mini-glass combination pH electrode (Hamilton Biotrode) coupled to a Fisher Accumet digital pH meter model 805 MP. pH Titrations were performed by adding small aliquots of concentrated solution of KOH to unbuffered solutions containing CdCl$_2$ (20−40 μM) and peptide (60−120 μM), and monitoring the change in absorbance at 235 nm as a function of pH. Equilibration time was always allowed before reading the final pH. In all cases, reverse titrations were carried out by adding small aliquots of concentrated solution of HCl to verify the reversibility of the process. The UV−vis pH titration curves of the peptides containing a single binding site were fit using the model and procedure published previously for the release of two protons upon Cd(II) binding to the three Cys thiolates.[41,42] The experimental data for the peptides **GRAND**-

(38) Nomenclature: While previously describing in detail the nomenclature for peptide modifications, we have not fully provided descriptors for metal complexation to these peptides. We will provide these definitions here with respect to Cd(II) and the exogenous ligand water; however, the nomenclature is general for any metal or non-protein bound ligand. We refer to an "apo peptide" as one which does not have metal in the designed metal coordination site within the hydrophobic interior of the coiled coils. We do not refer to an "apo peptide" to represent situations without the presence of any cofactors. Metals that may be bound non-specifically to the exterior hydrophilic residues are not considered to be metallated proteins/peptides in this context. Cd(II)-(TRIL16C)$_3^-$ indicates that Cd(II) is bound to the three stranded coiled coil; however, the metal coordination environment is either unknown or is a mixture of species (e.g., Cd(II)(TRIL16C)$_3^-$ contains a 55:45 mixture of CdS$_3$O and CdS$_3$, respectively). When the metal is placed within brackets, as in [Cd(II)(H$_2$O)](TRIL12AL16C)$_3^-$, we specify the coordination environment (in this case CdS$_3$O) and the possible exogenous ligand (here water). If the site has only protein ligands, then it would be represented as [Cd(II)](TRIL16Pen)$_3^-$. At low pH, one can encounter the situation where the cysteine sulfurs are protonated and may, or may not, be directly coordinated to the metal. In this case, we indicate this situation as [Cd(II)](TRIL16Pen[S,(SH)$_2$])$_3^-$ in which one cysteine is bound as a thiolate and the remaining two cysteines are protonated. When a peptide contains more than one binding site, we use the above nomenclature, but specify which site is being discussed by adding a superscript outside of the bracket to indicate the amino acid residues coordinating the specific metal (e.g., [Cd(II)][16][Cd(II)(H$_2$O)][30](GRANDL16PenL26AL30C)$_3^{-2}$). Finally, for cases where dual site peptides exhibit specificity for metal complexation, we will utilize [apo] to designate an empty site (e.g., [apo][16][Cd(II)(H$_2$O)][30](GRANDL16PenL26AL30C)$_3^-$).

(39) Chan, W. C.; White, P. D. *Fmoc Solid Phase Peptide Synthesis: A Practical Approach*; Oxford University Press: New York, 2000.

(40) Mantle, M.; Stewart, G.; Zayas, G.; King, M. *Biochem. J.* **1990**, *266*, 597−604.

(41) Matzapetakis, M.; Ghosh, D.; Weng, T.-C.; Penner-Hahn, J. E.; Pecoraro, V. L. *J. Biol. Inorg. Chem.* **2006**, *11*, 876−890.

L12AL16CL26AL30C and **GRAND**L16PenL19IL23PenL26I were fit using a model that was derived from the single binding site model, taking into account the two binding sites and the nonspecific binding of Cd(II), as it was observed in the [113]Cd NMR experiments (see Supporting Information for a full description of the model and the Results section for the [113]Cd NMR experiments). The same model was applied to fit the experimental data for the peptide **GRAND**L12AL16CL26AL30CL33I.

2.3. CD Spectroscopy. All Circular Dichroism data were collected using an Aviv model 202 thermostatically controlled Circular Dichroism Spectrometer equipped with a 450 W Xenon arc lamp. GuHCl titration experiments were carried out using a Microlab 500 series syringe pump automatic titrator controlled by Aviv software. Titrations were carried out by mixing two separate solutions of peptide containing 0.0 and 7.63 M GuHCl. Refractive index measurements were used to determine the concentration of the stock GuHCl solution.[43] Each of these solutions contained 10 μM monomer peptide and 10 mM phosphate buffer. The pH values were adjusted to 6.5 by adding KOH or HCl. Titrations were performed at 25 °C in a rectangular open top quartz cell of 1 cm path length. The observed ellipticity in millidegrees were plotted vs increasing GuHCl concentration. Whenever necessary, the data were fit by nonlinear least-squares methods to a two-state trimer-monomer equilibrium[44] using the software Igor Pro (Wavemetrics, Inc.). Midpoint values of the experimental curves were calculated from the concentration of GuHCl where the ellipticity is 50% from the starting ellipticity in the absence of denaturant.

2.4. [113]Cd NMR Spectroscopy. All of the spectra were collected at room temperature on a Varian Inova 500 spectrometer (110.92 MHz for [113]Cd) equipped with a 5 mm broadband probe. [113]Cd NMR spectra were externally referenced to a 0.1 M Cd(ClO$_4$)$_2$ solution in D$_2$O. A spectral width of 847 ppm (93 897 Hz) was sampled using a 5.0 μs 90° pulse and 0.05 s acquisition time with no delay between scans. Samples were prepared under a flow of argon by dissolving 30−35 mg of the lyophilized and degassed peptides in 450−500 μL 15% D$_2$O/H$_2$O solution. The peptide concentrations were determined by using the assay with 4,4′-dipyridyl disulfide,[40] and the concentrations range from 9 to 18 mM peptide, which corresponds to 3−6 mM three-stranded coiled coil. The final samples were prepared by the addition of the appropriate amount of 250 mM [113]Cd(NO$_3$)$_2$ solution (prepared from 95% isotopically enriched [113]CdO obtained from Oak Ridge National Laboratory) and the adjustment of the pH with KOH or HCl solutions. The pH value was measured both before and after the experiment. An argon atmosphere was maintained when possible but the samples came in contact with O$_2$ during addition of [113]Cd(NO$_3$)$_2$, pH adjustment, and acquisition. The data were analyzed using the software MestRe-C.[45] All free induction decays (FIDs) were zero filled to double the original points and were processed by application of 100 Hz line broadening prior to Fourier transformation.

2.5. ^{1}H NMR Spectroscopy. 2D ^{1}H NMR experiments were performed at room temperature on a 500 MHz Varian Inova spectrometer equipped with an inverse detection probe. Samples were prepared by dissolving 30−35 mg of lyophilized and degassed peptide in 500−600 uL 10% D$_2$O/H$_2$O under a flow of argon. Final solutions contained 3.0−4.0 mM of peptide trimer, as determined by the assay with 4,4′-dipyridyl disulfide.[40] Whenever necessary [113]Cd(II) was added in the form of 250 mM [113]Cd(NO$_3$)$_2$ stock solution and pH was adjusted with concentrated KOH or HCl solutions as described in the previous section. Attempts were made

(42) Iranzo, O.; Jakusch, T.; Lee, K.-H.; Hemmingsen, L.; Pecoraro, V. L. *Chem.−Eur. J.* **2009**, *15*, 3761−3772.

(43) Pace, C. N.; Scholtz, J. M. *Protein Structure: A Practical Approach*; Oxford University Press: Oxford, 1997.

(44) Boice, J. A.; Dieckmann, G. R.; Degrado, W. F.; Fairman, R. *Biochemistry* **1996**, *35*, 14480−14485.

(45) Cobas, C.; Cruces, J.; Sardina, F. J. *MestRe-C*, 2.3 ed.; Universidad de Santiago de Compostela, Spain, 2000.

Table 3. Parameters Fitted to the PAC Data[a]

peptide ($c_{Cd(II)}/c_{peptide\ monomer}$)	pH	ω_0 (rad/ns)	η	$\Delta\omega_0/\omega_0$ ($\times$ 100)	$1/\tau_c$ (μs^{-1})	A ($\times$ 100)	population[c] (%)	χ_r^2
GRANDL26AL30C	7.0	0.348(1)	0.12(2)	1.5(5)	3.6(5)	1.8(2)	21	1.19
(1/12)		0.245(3)	0.30(3)	12(2)	3.6(5)	5.1(7)	61	
		0.107(9)[b]	0.57(9)	15[d]	3.6(5)	1.5(3)	18	
GRANDL26AL30C	9.1	0.347(1)	0.10(2)	1.4(5)	2.2(4)	1.7(2)	19	1.29
(1/12)		0.243(3)	0.31(3)	14(2)	2.2(4)	7.4(6)	81	
GRANDL16PenL26AL30C	6.5	0.347(2)	0.05(8)	2.3(3)	4.2(5)	1.8(3)	17	1.15
(1/12)		0.245(3)	0.32(3)	12(2)	4.2(5)	6.5(8)	61	
		0.105(7)[b]	0.59(7)	15[d]	4.2(5)	2.3(3)	22	
GRANDL16PenL26AL30C	9.3	0.345(1)	0.10(3)	0.5(5)	5.9(7)	1.7(3)	17	1.11
(1/12)		0.247(3)	0.26(3)	12(2)	5.9(7)	7.2(7)	72	
		0.159(8)[b]	0.77(5)	0(4)	5.9(7)	1.1(4)	11	
GRANDL16PenL26AL30C	9.3	0.457(2)	0.0(5)	1.9(6)	7.5(1)	2.3(3)	29	1.23
(1.85/3)		0.349(2)	0.0(3)	0.4(8)	7.5(1)	0.9(2)	11	
		0.255(4)	0.22(5)	9(2)	7.5(1)	3.4(5)	43	
		0.125(9)[b]	0.4(1)	12(6)	7.5(1)	1.3(3)	16	
GRANDL16PenL19IL23PenL26I	9.2	0.461(1)	0.02(4)	0.7(3)	17(2)	6.8(3)	100	1.44
(1.85/3)[e]								
GRANDL12AL16CL26AL30C	8.7	0.342(6)	0.148(8)	1.8(3)	3.8(6)	5.3(3)	55	1.08
(1.85/3)		0.242(8)	0(1)	16(4)	3.8(6)	3.9(8)	40	
		0.142(2)[b]	0.1(2)	0(2)	3.8(6)	0.5(2)	5	

[a] The numbers in parentheses are the standard deviations of the fitted parameters. [b] Including this NQI significantly improves the fit, but at least two different parameter sets give equally good fits - one possible set of parameters is presented here. [c] The relative population of each species determined using the amplitudes in this Table. [d] Fixed in the fit. [e] Although the stoichiometry implies that two sites are occupied, the χ_r^2 is not reduced significantly upon inclusion of a second NQI in the fit, and it was not possible to reliably derive parameters for two individual NQIs.

to keep an argon atmosphere throughout, but the samples did come into contact of air during addition of ^{113}Cd(NO$_3$)$_2$, pH adjustment and data acquisition. Nuclear Overhauser Effect Spectroscopy (NOESY) experiments were performed using standard Varian pulse sequences with mixing time of 100 ms.[46] For water suppression, presaturation was used for 1.5 s with saturation power of 5 dB.[47] A spectral window of 11.2 ppm was sampled with 2048 points and 256 increments in the indirect dimension with 8 scans. Z-gradient Total Correlation Spectroscopy (ZTOCSY) experiment was performed only for the apo peptide under similar conditions with spin lock field strength of 7 kHz for the 90° pulse.[48] An 80 ms spin lock was used during the experiment. All of the data were processed by MestRe Nova.[49]

2.6. ^{111m}Cd Perturbed Angular Correlation (PAC) Spectroscopy. All ^{111m}Cd PAC experiments and sample preparation were performed as described previously.[42,50,51] The final volume of the samples ranged between 0.05 and 0.5 mL with concentrations of 250−300 μM peptide, 20 mM appropriate buffer (MES for pH values 6.5 and 7.0, and CHES for pH values between 8 and 9.3) and different Cd(II)/peptide ratios (Table 3). All fits were carried out with 300 data points, disregarding the first 5 points due to systematic errors in these. All PAC spectra were initially analyzed with four NQIs (vide infra), and NQIs were included in the fit if the amplitude was larger than two times the standard deviation. Each nuclear quadrupole interaction (NQI) was modeled using a separate set of parameters that includes ω_0, η, $\Delta\omega_0/\omega_0$, $1/\tau_c$, and A. The parameter ω_0 ($\omega_0 = 12\pi|eQV_{zz}|/(40\ h)$, where Q is the nuclear electric quadrupole moment and V_{zz} is the numerically largest component of the diagonalized electric field gradient tensor) is associated with the strength of the interaction between the surrounding charge distribution and the Cd nucleus, η is the so-

called asymmetry parameter which is 0 in an axially symmetric complex and has a maximal value of 1; $\Delta\omega_0/\omega_0$ describes static structural variations from one Cd(II) site to the next, and is as such a measure of the structural variability; τ_c is the rotational correlation time; and A is the amplitude of the signal (see ref 32 for a more detailed description). The rotational correlation time was constrained to be the same for all NQIs in a given spectrum. The parameters fitted to the PAC data are presented in Table 3. In two cases $\Delta\omega_0/\omega_0$ was fixed to 15%, denoted with "d" in Table 3. Setting the parameter free in the fit led to very large values, and fixing it did not alter the reduced χ-square.

3. Results

3.1. Cd(II) Binding to the GRAND Peptides. The stoichiometry and the pH dependence of the binding of Cd(II) to the **GRAND** peptides were monitored by UV−vis spectroscopy using the ligand-to-metal charge-transfer (LMCT) band at 235 nm corresponding to the formation of Cd−S bonds in CdS$_3$ or CdS$_3$O complexes.

3.1.1. Stoichiometry. The addition of Cd(II) aliquots into the different solutions containing 60 μM (20 μM trimer) **GRAND** peptides at pH values where, based on the pH titrations, the peptides are capable of fully binding the Cd(II), generated the appearance of the characteristic LMCT. Shown in Figure 1 are the titration curves obtained by plotting the increase in absorbance vs the equivalents of Cd(II) added per trimer of **GRAND** peptides. In all cases, the curves plateau at 2($\pm$0.14) equiv of Cd(II). The different observed final absorbance values reflect the higher extinction coefficient of the 3-coordinated CdS$_3$ species compared to the 4-coordinate CdS$_3$O species at 235 nm.[34,36]

3.1.2. pH Dependence. The increase in pH of a solution containing 40 μM Cd(II) and 60 μM (20 μM trimer) **GRAND**L16PenL19IL23PenL26I enhances the 235 nm LMCT transition with Figure 2 showing this pH titration curve (green). The equivalent titration curve with **GRAND**-L12AL16CL26AL30C is shown in blue indicating binding of Cd(II) at lower pH values. The shape of these pH titration curves

(46) Jeener, J.; Meier, B. H.; Bachmann, P.; Ernst, R. R. *J. Chem. Phys.* **1979**, *71*.
(47) Hoult, D. I. *J. Magn. Reson.* **1976**, *21*, 337–347.
(48) Rance, M. *J. Magn. Reson.* **1987**, *74*, 557–564.
(49) *MestReNova*, version 6.XX, Mestrelab Research S.L., Santiago de Compostela, Spain, www.mestrelab.com, 2009.
(50) Hemmingsen, L.; Bauer, R.; Bjerrum, M. J.; Zeppezauer, M.; Adolph, H. W.; Formicka, G.; Cedergren-Zeppezauer, E. *Biochemistry* **1995**, *34*, 7145–7153.
(51) Hemmingsen, L.; B., R.; Bjerrum, M.; Adolph, H.; Zeppezauer, M.; Cedergren-Zeppezauer, E. *Eur. J. Biochem.* **1996**, *241*, 546–551.
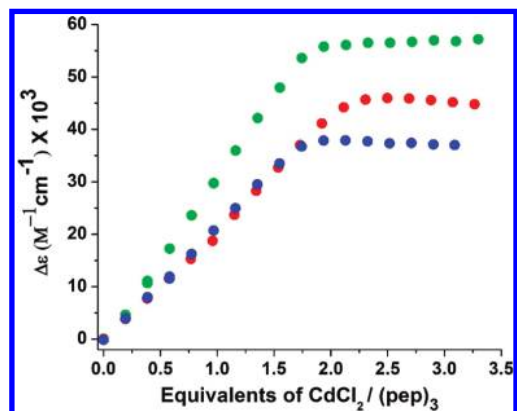
Figure 1. Titration curves obtained by plotting the change in the absorbance at 235 nm as a function of the equivalents of CdCl$_2$ added to solutions containing 20 μM (**GRAND**L16PenL26AL30C)$_3$ at pH 9.0 (red), 20 μM (**GRAND**L12AL16CL26AL30C)$_3$ at pH 8.6 (blue), and 20 μM (**GRAND**-L16PenL19IL23PenL26I)$_3$ at pH 9.5 (green). All of the curves plateau at 2 $\pm$ 0.14 equiv of CdCl$_2$ per equiv of peptide trimer.
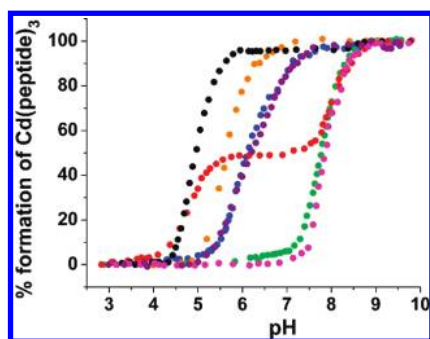

Figure 2. pH dependence of the binding of 2 equiv of CdCl$_2$ to 20 μM (**GRAND**L16PenL26AL30C)$_3$ (red), (**GRAND**L12AL16CL26AL30C)$_3$ (blue), (**GRAND**L16PenL19IL23PenL26I)$_3$ (green), (**GRAND**L12AL16CL26-AL30CL33I)$_3$ (purple) and of 1 equiv of Cd(II) to 20 μM (**GRAND**-L26AL30C)$_3$ (black), (**GRAND**L12AL16C)$_3$ (orange) and (**GRAND**-L16Pen)$_3$ (magenta). UV/vis absorbance due to LMCT band at 235 nm was monitored during the course of titration and is plotted as normalized absorbance vs pH.

is consistent with the release of four protons upon binding of 2 equiv of Cd(II) and, therefore, it is in agreement with our published model for the simultaneous release of the final two protons upon Cd(II) binding to the remaining two thiolates of either Cys or Pen ([Cd(pep)(Hpep)$_2$]$^+$ species to give the [Cd(pep)$_3$]$^-$).[41,42] However, unlike the pH titration curve obtained for the peptide **GRAND**L16PenL26AL30C (Figure 2, red), where two well-defined regions were observed allowing for the independent analysis of both sites,[36] only one inflection point was obtained for the peptides **GRAND**L16PenL19IL-23PenL26I and **GRAND**L12AL16CL26AL30. These results point out that in these **GRAND** peptides both sites bind Cd(II) at similar pH values. In these cases, and taking into account the ^{113}Cd NMR pH titrations (see below), the experimental data were fit to a model where binding of 2 equiv of Cd(II) occurs simultaneously to both sites (see Experimental Section and SI for the full description). The resulting pK_{a2} values are reported in Table 2.

3.2. CD Spectroscopy. The stabilities of the peptides **GRAND**L26AL30C, **GRAND**L12AL16C, **GRAND**L12AL16-CL26AL30C, and **GRAND**L12AL16CL26AL30CL33I were assessed from their GuHCl-induced unfolding titration curves at pH 6.5. The observed ellipticity in millidegrees as a function of denaturant concentration was plotted to generate the titration
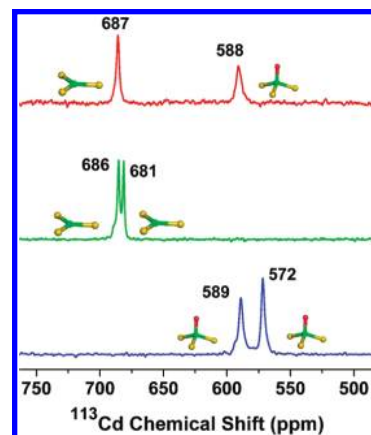

Figure 3. ^{113}Cd NMR spectra of 3.0 mM [Cd(II)]^{16}[Cd(II)(H$_2$O)]^{30}-(**GRAND**L16PenL26AL30C)$_3$$^{2-}$ at pH 9.6 (red), 3.4 mM [Cd(II)]$_2$-(**GRAND**L16PenL19IL23PenL26I)$_3$$^{2-}$ at pH 9.5 (green) and 3.3 mM [Cd(II)(H$_2$O)]$_2$(**GRAND**L12AL16CL26AL30C)$_3$$^{2-}$ at pH 8.5 (blue). Ball and stick models show the coordination environments of 3- and 4-coordinate Cd(II) complexes. Yellow spheres represent S atoms of Cys/Pen with the green and red spheres representing Cd(II) ion and water molecule, respectively.

curves (Figure S2 of the SI). **GRAND**L26AL30C with a denaturation midpoint of 3.7 M (magenta) shows that this is the most stable construct followed by **GRAND**L12AL16C (midpoint 3.3 M, red), **GRAND**L12AL16CL26AL30CL33I (midpoint 2.9 M, green), and **GRAND**L12AL16CL26AL30C (midpoint 1.7 M, blue). The shape of the denaturation titration curve for **GRAND**L12AL16CL26AL30CL33I is different from the other peptides, which suggests that the Ile group has most likely modified the trimer-monomer two state equilibrium. Fits to the experimental curves were performed as described in the Experimental Section for the peptides **GRAND**L26AL30C, **GRAND**L12AL16C, and **GRAND**L12AL16CL26AL30C only (Table S1, Figure S2 of the SI).

3.3. ^{113}Cd NMR Spectroscopy. The ^{113}Cd NMR spectra of **GRAND**L16PenL19IL23PenL26I (Figure 3, green) and **GRAND**-L12AL16CL26AL30C (Figure 3, blue) were recorded in the presence of 2 equiv of ^{113}Cd(NO$_3$)$_2$ at pH 9.5 and 8.5, respectively. Two resonances were observed in each case with chemicals shifts of 686 and 681 ppm for **GRAND**L16-PenL19IL23PenL26I, and 589 and 572 ppm for **GRAND**-L12AL16CL26AL30C. ^{113}Cd NMR pH titrations were carried out for both peptides. The pH of a solution containing 3.0 mM (**GRAND**L16PenL19IL23PenL26I)$_3$ and 2 equiv of ^{113}Cd(NO$_3$)$_2$ was varied from pH 7.5 to 9.5 and the ^{113}Cd NMR recorded (Figure 4A). Three resonances were observed at pH 7.5 with chemical shifts of 681, 686, and 691 ppm. An increase in pH led to decreased intensity of the resonance at 691 ppm and an increase of the resonance at 681 ppm. The resonance at 686 ppm increased continuously. By pH 9.5, only the resonances at 681 and 686 ppm were observed. The analogous experiment with 3.0 mM (**GRAND**L12AL16CL26AL30C)$_3$ and 2 equiv of ^{113}Cd(NO$_3$)$_2$ was carried out between pH 6.0 and 8.5 (Figure 5). All of the spectra showed two resonances with chemical shifts of 589 and 572 ppm. The ^{113}Cd NMR spectrum of 3.3 mM (**GRAND**L12AL16CL26AL30C)$_3$ in the presence of 1.0 equiv of ^{113}Cd(NO$_3$)$_2$ at pH 6.0 showed a single resonance at 572 ppm (Figure S3 of the SI). To determine if these peptides show site-selective binding of Cd(II), experiments were carried out where an aliquot of 1.0 equiv of ^{113}Cd(NO$_3$)$_2$ was added to a solution containing 3.3 mM (**GRAND**L16PenL19IL23-PenL26I)$_3$ at pH 9.5 or 3.0 mM (**GRAND**L12AL16CL26AL-
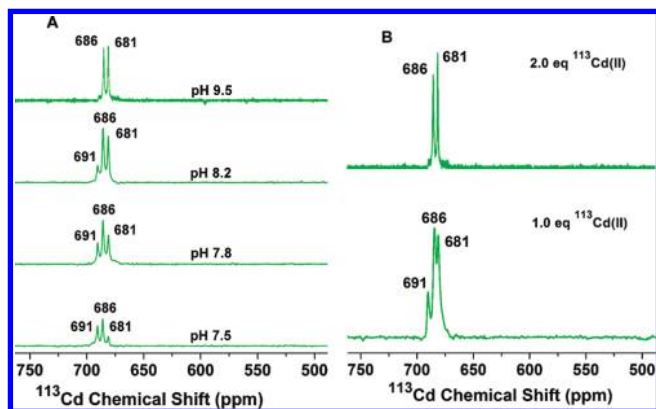
Figure 4. [113]Cd NMR spectra of solutions containing (**A**) 3.0 mM (**GRAND**L16PenL19IL23PenL26I)₃ and 2 equiv of [113]Cd(NO₃)₂ at different pH values, and (**B**) 3.3 mM (**GRAND**L16PenL19IL23PenL26I)₃ loaded with 1 and 2 equiv of [113]Cd(NO₃)₂ at pH 9.5.

Figure 5. [113]Cd NMR spectra of solutions containing 3.3 mM (**GRAND**L12AL16CL26AL30C)₃ and 2 equiv of [113]Cd(NO₃)₂ at different pH values. (The most downfield peaks marked by the asterisks are impurities).

30C)₃ at pH 8.5. Three resonances with chemical shifts of 681, 686, and 691 ppm were observed for **GRAND**L16PenL19IL-23PenL26I (Figure 4B), similar to those observed at low pH under stoichiometric conditions. For **GRAND**L12AL16CL-26AL30C, the [113]Cd NMR spectrum (Figure S4) showed two peaks at 589 and 572 ppm.

3.4. [111m]Cd PAC Spectroscopy. [111m]Cd PAC spectroscopy was used to determine the Cd(II) coordination geometry of the different complexes [Cd(II)(H₂O)](**GRAND**L26AL30C)₃⁻, [Cd(II)][16][Cd(II)(H₂O)][30](**GRAND**L16PenL26AL30C)₃²⁻, [Cd-(II)(H₂O)]₂(**GRAND**L12AL16CL26AL30C)₃²⁻, and [Cd(II)]₂-(**GRAND**L16PenL19IL23PenL26I)₃²⁻. The [111m]Cd PAC spectra obtained are shown in Figure 6. The PAC data were analyzed as described in the Experimental Section and the fitted parameters are reported in Table 3. The observed values of ω_0, giving information regarding the first coordination sphere ligands, fall into four frequency regions: (1) NQI1: high frequency signal ($\omega_0 \approx 0.457-0.461$ rad/ns) assigned to a trigonal CdS₃ structure;[32,34] (2) NQI2: ($\omega_0 \approx 0.342-0.349$ rad/ns) assigned to a tetrahedral CdS₃X structure (where X may be H₂O);[32,34] (3) NQI3: ($\omega_0 \approx 0.242-0.255$ rad/ns) probably reflecting a coordination geometry with 2−3 Cys and 1−2 other N or O containing ligands; and (4) NQI4: a low frequency signal ($\omega_0 \approx 0.105-0.159$ rad/ns giving rise to a broad feature around 0.140−0.200 rad/ns in the spectra) which is present in almost
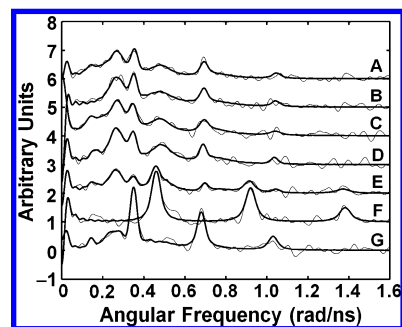

Figure 6. [111m]Cd PAC spectra of the different **GRAND** peptides [Fourier transform: experimental data (thin line) and fits (bold faced line) are shown overlaid]. All the samples contained 20 mM appropriate buffer and 250−300 μM peptide. (**A**) **GRAND**L26AL30C, 1/12 equiv Cd(II), pH 7.0; (**B**) **GRAND**L26AL30C, 1/12 equiv Cd(II), pH 9.1; (**C**) **GRAND**L16PenL-26AL30C, 1/12 equiv Cd(II), pH 6.5; (**D**) **GRAND**L16PenL26AL30C, 1/12 equiv Cd(II), pH 9.3; (**E**) **GRAND**L16PenL26AL30C, 1.85/3 equiv Cd(II), pH 9.3; (**F**) **GRAND**L16PenL19IL23PenL26I, 1.85/3 equiv Cd(II), pH 9.2; and (**G**) **GRAND**L12AL16CL26AL30C, 1.85/3 equiv Cd(II), pH 8.7.

all spectra and likely represents one or several Cd(II) nonspecifically bound species coordinated to the carboxylate groups at the interface of the helices forming the coiled coils. This NQI4 represents only a minor fraction of the signal and, therefore, it is difficult to obtain a good fit of the PAC parameters. Since it is a small and common feature in the spectra, we will not comment on it further.

The PAC spectrum of **GRAND**L26AL30C with 1/12 Cd(II)/peptide ratio at pH 7.0 shows the signatures corresponding to NQI2 ($\omega_0 = 0.348$ rad/ns) and NQI3 ($\omega_0 = 0.245$ rad/ns). Also, a minor fraction of NQI4 was observed. A very similar spectrum was obtained for the same peptide with 1/12 Cd(II)/peptide ratio at pH 9.1 (Figure 6) and the fitting of the experimental data gave the same prominent NQIs (NQI2 and NQI3, Table 3). NQI4 was not significantly present in this data set. The PAC spectra of **GRAND**L16PenL26AL30C with 1/12 Cd(II)/peptide ratio at pH 6.5 and 9.3 are highly similar to those observed for **GRAND**L26AL30C and can be analyzed with essentially the same NQIs (NQI2, NQI3, and NQI4) with minor variations in the relative amplitudes. When at pH 9.3, the ratio of Cd(II) to peptide was increased to achieve the loading of both binding sites (1.85/3 Cd(II)/peptide ratio), the high frequency signal (NQI1) appeared in addition to the features corresponding to the three NQIs found at low Cd(II)/peptide ratio (Figure 6). Thus, the data indicate that the CdS₃ site is only occupied at high Cd(II)/peptide ratios. The PAC spectra obtained for the **GRAND**L12AL16CL26AL30C peptide at pH 8.7 under conditions that favor loading of both binding sites (1.85/3 Cd(II)/peptide ratio) gives a PAC signal with the signature of the L26AL30C site but with a more prominent NQI2 ($\omega_0 = 0.342$ rad/ns). The origin of this increase in amplitude for NQI2 is attributed to the binding of Cd(II) to the L12AL16C site, which is supported by the fact that Cd(II) binds to this site as a single CdS₃O species (as observed for **TRI**L12AL16C).[34] Interestingly, all peptides investigated with PAC spectroscopy in this work and containing the L26AL30C site display this signature: a mixture of NQI2, NQI3, and possibly NQI4 (minor fraction), suggesting structural variability. The PAC spectrum of the peptide **GRAND**L16PenL19IL23PenL26I recorded at pH 9.2 and high Cd(II) concentration (1.85/3 Cd(II)/peptide ratio, Figure 6) shows a single prominent signal in the high frequency range. Since this high frequency signal can be fitted with just one NQI, corresponding to NQI1 (trigonal CdS₃), the two binding sites
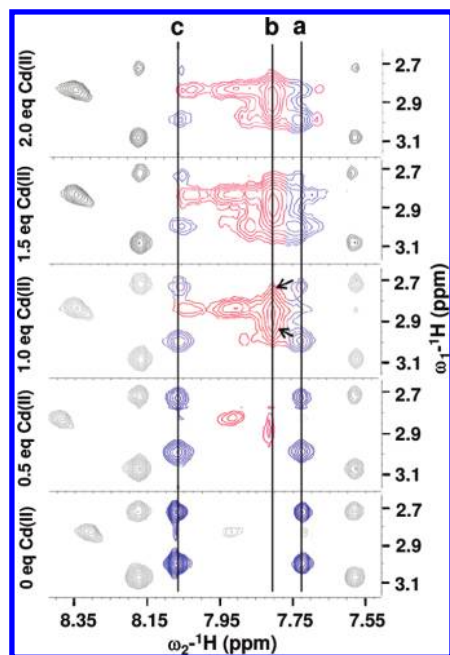
Figure 7. Sections of $^1H-^1H$ NOESY spectra of 3.25 mM (**GRAND**L12AL16CL26AL30C)$_3$ as a function of added equivalents of Cd(II) at pH 6.0. Peak at 7.91 ppm corresponds to H^N of E21 and other peaks displayed in gray correspond to interesidue NOEs (H^N_i–H$^\beta_{i+1}$) (see text for full description). Colored peaks correspond to intraresidue NOEs of the amide protons (H^N, vertical axis) and the β-methylene protons (H$^\beta$, horizontal axis) of Cys: (a) H$^N_{16}$–H$^\beta_{16}$ for **GRAND**L12AL16CL26AL30C; (b) H$^N_{16}$–H$^\beta_{16}$ for [Cd(II)(H$_2$O)]^{16}[apo]^{30}(**GRAND**L12AL16CL26-AL30C)$^-$; and (c) H$^N_{30}$–H$^\beta_{30}$ for **GRAND**L12AL16CL26AL30C.

in the triple helix formed by this peptide appear to have highly similar structures.

3.5. ^1H NMR Spectroscopy. To ascertain the site specificity of Cd(II) binding to **GRAND**L12AL16CL26AL30C at pH 6.0 further, we used two-dimensional NMR spectroscopy. The backbone resonances of the peptide were assigned using NOESY and TOCSY spectra, (Figure S5 shows the sequential assignment of amide protons (H^N) of Glu7 to Leu33). Using this information, β-methylene protons (H$^\beta$) of each Cys residues were identified. NOESY spectra were used to monitor the progress of Cd(II) titration into 3.25 mM (**GRAND**L12AL16CL-26AL30C)$_3$ at pH 6.0 by observing changes in the H^N–H$^\beta$ cross peak region of Cys (Figure 7). The horizontal axis in Figure 7 corresponds to the H^N and the vertical axis corresponds to the H$^\beta$ of each Cys. Two nonequivalent H$^\beta$ appear as separate cross peaks corresponding to each H^N. The regions **a** (7.72 ppm) and **c** (8.07 ppm) of Figure 7 correspond to cross peaks of H$^N_{16}$–H$^\beta_{16}$ and H$^N_{30}$–H$^\beta_{30}$, respectively. Two sets of additional cross peaks at 7.57 ppm and 8.17 ppm correspond to interesidue cross peaks between H^N of Lys17 and H$^\beta$ of Cys16 and between H^N of Lys31 and H$^\beta$ of Cys30, respectively. These peaks contain redundant information as regions **a** and **c** in the figure and will not be considered further. The cross peak at 7.91 ppm can be best assigned as H^N–H$^\gamma$ cross peak of Glu21. After the addition of 0.5 and 1.0 equiv of ^{113}Cd(NO$_3$)$_2$ the major cross peak at 7.81 ppm appears, marked as region **b**. This new peak is broad along the F1 dimension and is an overlap of the two individual H$^\beta$ resonances of Cys16 which are perturbed due to Cd(II) binding to Cys16. These results display preferential binding of Cd(II) to the Cys16 site at pH 6.0. From 1.0 to 2.0 equiv of Cd(II), the cross peak at 8.03 ppm appears that corresponds to perturbations of the H^N–H$^\gamma$ of Glu21 resonance upon addition

of Cd(II). From 1.5 to 2.0 equiv of added Cd(II), a cross peak at 7.86 ppm appears which may represent the perturbation of the Cys30 resonance due to interaction of Cd(II) with the partially deprotonated Cys30 at pH 6.0. To ascertain that region **b** in Figure 7 represents the cross peaks due to Cd(II) binding to the Cys16 and not to the Cys30 site, a series of pH dependent NOESY experiments were performed. The pH of a solution containing 3.21 mM (**GRAND**L12AL16CL26AL30C)$_3$ and 2.0 equiv of Cd(II) was increased from 6.0 to 8.5 (Figure S6 of the SI). With an increase in pH, two new cross peaks appear at 7.6 ppm (region **d**) and 7.93 ppm (region **e**). These resonances are assigned as H$^N_{16}$–H$^\beta_{16}$ for [Cd(II)(H$_2$O)]$_2$(**GRAND**L12AL16-CL26AL30C)$_3^{2-}$ (region **d**) and H$^N_{30}$–H$^\beta_{30}$ for [Cd(II)-(H$_2$O)]$_2$(**GRAND**L12AL16CL26AL30C)$_3^{2-}$ (region **e**). The cross peak at 7.81 ppm (region **b**) remains at high pH (8.5) indicating the presence of the species [Cd(II)(H$_2$O)]^{16}[apo]^{30}-(**GRAND**L12AL16CL26AL30C)$_3^{4-}$ in solution. This result demonstrates that the new cross peaks are associated with Cd(II) binding to the less acidic Cys30 site and that the cross peak at region **b** in Figure 7 results from Cd(II) binding to the more acidic Cys16 site.

4. Discussion

The objective of this work is to assess whether the position of metal sites along the linear sequence of the peptide influences, possibly fine-tuning, the physical properties of the bound metal ions. Secondly, we wanted to assess whether the presence of a second bound metal influenced the properties of the first coordinated metal. To address these issues, we designed peptides capable of binding 2 equiv of Cd(II) with identical coordination geometries and evaluated the physical properties of the bound ions, the selectivity of the metals for the different sites and the influence of pH on the observed properties. While other studies have shown that de novo peptides can bind two metal ions in separate mononuclear sites[52,53] or in binuclear centers,[54–56] they did not address the question of selective binding of the same metal ion in different centers having similar geometries. The model peptides used to test these issues are **GRAND**L12AL16-CL26AL30C, designed to have two 4-coordinate sites (CdS$_3$O) and **GRAND**L16PenL19IL23PenL26I with two 3-coordinate sites (CdS$_3$). Since these sites are located at different positions in the coiled coil, the final Cd(II) constructs perfectly evaluate how metal positioning influences their physical properties. Thus, we may assess whether or not Cd(II) displays site-selective binding, whether the binding of one metal in a helix alters the properties of the second metal and whether the spectral properties of a bound Cd(II) are dependent on the proximity to the center or ends of a helical bundle. These important issues are yet to be addressed with designed peptides.

4.1. Designing a Peptide With Dual 3-Coordinate Sites. Our first challenge was designing the Cys substituted **GRAND** peptides. To guide our designs, we have used the linear

(52) Matzapetakis, M.; Pecoraro, V. L. *J. Am. Chem. Soc.* **2005**, *127*, 18229–18233.
(53) Tanaka, T.; Mizuno, T.; Fukui, S.; Hiroaki, H.; Oku, J.-i.; Kanaori, K.; Tajima, K.; Shirakawa, M. *J. Am. Chem. Soc.* **2004**, *126*, 14023–14028.
(54) Lombardi, A.; Summa, C. M.; Geremia, S.; Randaccio, L.; Pavone, V.; DeGrado, W. F. *Proc. Natl. Acad. Sci., U.S.A.* **2000**, *97*, 6298–6305.
(55) Summa, C. M.; Rosenblatt, M. M.; Hong, J.-K.; Lear, J. D.; DeGrado, W. F. *J. Mol. Biol.* **2002**, *321*, 923–938.
(56) Spiegel, K.; De Grado, W. F.; Klein, M. L. *Proteins: Struct., Funct., Bioinf.* **2006**, *65*, 317–330.

Table 4. % Cd(II) Species (4-Coordinate and 3-Coordinate) Based on ^{113}Cd NMR Chemical Shift Values and the ^{113}Cd NMR−^{111m}Cd PAC Spectroscopic Correlation[a]

peptide	^{113}Cd NMR δ (ppm)	% Cd species 4-coordinate (CdS$_3$O)	% Cd species 3-coordinate CdS$_3$
GRANDL12AL16CL23Pen	575	100	0
	640	55	45
GRANDL16PenL23PenL26I	678	20	80
	666	29	71
GRANDL16PenL19IL23PenL26I	686	13	87
	681	17	83
GRANDL12AL16CL26AL30C	572	100	0
	589	92	8

[a] Chemical shifts of 579 and 702 ppm are used as values corresponding to a 100% 4-coordinate and 3-coordinate Cd(II) species, respectively.[42]

correlation between the ^{113}Cd NMR and ^{111m}Cd PAC spectroscopy.[42] We began with the preparation of the peptide containing two 3-coordinate sites. On the basis of our previous results, positions near the edge of the coiled coil should be avoided in order to obtain a 3-coordinate site.[33,34,36] These positions are prone to coordinate water due to the fraying of the α-helices and thus, both binding sites should be buried in the interior of the coiled coil. The starting point for the design was our peptide **GRAND**L16PenL26AL30C known to contain one 3-coordinate site and one 4-coordinate site (Figure 3, red).[36] Our first strategy was to keep the Pen residue in position 16, since we know this location generates a 3-coordinate site,[34] and introduce the second Pen as far as possible from the C-terminal edge to avoid fraying, but separate enough from the first one to avoid the disruption of this site. On the basis of these requisites, the second Pen could be introduced into position 23 (fourth heptad repeat); however, making a peptide containing two separate binding sites that can encapsulate two Cd(II) ions as 3-coordinate complexes at both the binding sites is not so straightforward as simply adding a Pen to an interior site as a construct previously synthesized in our group, **GRAND**L12AL16CL23Pen (unpublished results) bound Cd(II) in position 23 as a mixture of species (55% CdS$_3$O and 45% CdS$_3$, Table 4). Since moving the Pen toward the interior of the coiled coil could disrupt the first binding site, we decided to substitute Leu26 for an Ile. This residue is known to pack better and should prevent fraying by generating a more compact packing of the α-helices. The ^{113}Cd NMR spectra of the resulting construct, **GRAND**L16-PenL23PenL26I, loaded with 2 equiv of Cd(II) at pH 9.6 exhibited two distinct peaks, with chemical shifts of 678 and 666 ppm. These values revealed the disruption of the first Pen site (L16Pen) by the introduction of the second site (L23Pen) since a ^{113}Cd chemical shift of 685 ppm was observed for the original fully 3-coordinate 16Pen site.[34,36] While the chemical shifts obtained represented an improvement toward the achievement of fully 3-coordinate sites, they indicate an equilibrium between CdS$_3$ and CdS$_3$O (678 ppm ≈ 80:20 and 666 ppm ≈ 71:29, Table 4). We have used the ^{113}Cd NMR shifts to assess the degree of formation of the CdS$_3$, but this method could provide a slight underestimate of the amount present. The existence of a single Leu layer between these two sites seemed to be insufficient to keep a compact packing and avoid perturbation of the 16Pen site due to the presence of the 23Pen site. To improve these results and minimize the disruption of the 16Pen site, the Leu layer just below (Leu19) was replaced by Ile. This generates an even more compact packing of the hydrophobic core. Indeed, this strategy succeeded as

GRANDL16PenL19IL23PenL26I bound 2(±0.14) equiv of Cd(II) with trigonal planar CdS$_3$ geometries (686 (CdS$_3$:CdS$_3$O ≈ 87:13, Table 4) and 681 (CdS$_3$:CdS$_3$O ≈ 83:17, Table 4) ppm) as shown in Figure 3 (green).

4.2. Designing a Peptide With Dual 4-Coordinate Sites. Our starting point for designing the peptide containing two 4-coordinate sites was again the construct **GRAND**L16PenL-26AL30C.[36] In this case, we kept the segment containing the 4-coordinate site (L26AL30C) and modified the L16Pen center, known to generate a 3-coordinate site,[34] to an L12AL16C center to obtain the second 4-coordinate site. Previous work with **TRI**L12AL16C suggested that this would be a successful approach.[34] This design yields the final peptide **GRAND**-L12AL16CL26AL30C. The binding of Cd(II) was characterized by ^{113}Cd NMR spectroscopy and the spectrum of the fully loaded [Cd(II)(H$_2$O)]$_2$(**GRAND**L12AL16CL26AL30C)$_3$$^{2-}$ showed two resonances at 589 (CdS$_3$:CdS$_3$O ≈ 8:92, Table 4) and 572 (CdS$_3$: CdS$_3$O ≈ 0:100, Table 4) ppm. These chemical shifts are consistent with those expected for a CdS$_3$O environment,[42] demonstrating that we successfully designed a single peptide with two 4-coordinate centers.

4.3. GRANDL16PenL19IL23PenL26I Peptide.

4.3.1. Physical Properties. With the two desired **GRAND** peptides in hand, we next investigated the impact that the position of the centers has on the intrinsic physical properties of the metal ion. Titration of Cd(II) into a solution containing 60 μM (20 μM trimer) **GRAND**L16PenL19IL23PenL26I at pH 9.5 was accompanied by an absorption increase centered at 235 nm and a final extinction coefficient of 54 772 M^{-1}cm^{-1}, which is consistent with the formation of two Cd(II) tris thiolate chromophores. The titration curve shown in Figure 1 (green color) indicates that the stoichiometry of peptide to Cd(II) is 3:2(±0.14) and, therefore, the best description for the Cd(II) complex formed under these conditions is [Cd(II)]$_2$(**GRAND**-L16PenL19IL23PenL26I)$_3$$^{2-}$. As discussed above, based on the ^{113}Cd NMR spectrum (Figure 3, green) these two Cd(II) sites are trigonal CdS$_3$. Further support for this assignment comes from the ^{111m}Cd PAC spectrum of [Cd(II)]$_2$(**GRAND**L16Pen-L19IL23PenL26I)$_3$$^{2-}$ (Figure 6F). This dicadmium peptide has a high frequency signal (NQI1) with parameters ω_0 = 0.461(1) rad/ns and η = 0.02(4) (Table 3) that correspond to a trigonal planar CdS$_3$ geometry with highly similar structures, indicating that the two sites created in (**GRAND**L16PenL19IL23PenL26I)$_3$ yield two metal ion sites with no indication of CdS$_3$O.

We have previously discriminated CdS$_3$ and CdS$_3$O sites in **TRI** and **GRAND** peptides by examining the pH profile for the formation of the tris cysteine complexes. In these cases, the relevant equilibrium is as follows: [Cd(pep)(Hpep)$_2$]$^+$ → [Cd(pep)$_3$]$^-$ + 2H$^+$. We have found that CdS$_3$ complexes (using Pen or Cys) have effective pK_{a2} values that are far more basic than the comparable CdS$_3$O structures (e.g., **TRI**L16Pen, pK_{a2} = 15.8 vs **TRI**L12AL16C, pK_{a2} = 12.2).[42] The pH profile for the binding of the 2 equiv of Cd(II) to this peptide (Figure 2) is consistent with these results since the pK_{a2} values obtained, 15.2 and 15.9, are very similar and quite basic as is expected for 3-coordinate sites. On the basis of previous observations, we infer that the site with the ^{113}Cd NMR shift of 686 ppm has the more basic of these pK_{a2} values as it has virtually no CdS$_3$O present. All of these data demonstrate that we have prepared a single peptide capable of binding 2 equiv of Cd(II) with trigonal planar CdS$_3$ coordination. The fact that the physical properties observed for both sites are comparable indicates that the location of the 3-coordinate site in the coiled coil is not perturbing or

fine-tuning its intrinsic properties. Furthermore, at this point it appears that in a well packed helix, the presence of the second CdS_3 center has minimal impact on the original chromophore (i.e., vs **GRAND**L16Pen). This latter point will now be addressed in more detail.

4.3.2. Does the Metalation State of One Site Perturb the Other Site? Now we will focus on the two related experiments performed with the **GRAND**L16PenL19IL23PenL26I peptide as shown in Figure 4. In the following section, we will discuss the possible interpretations of the data presented in Figure 4A,B in a systematic way. We will refer to the site with chemical shift of 686 ppm as site A and the site with chemical shift of 681 ppm as site B. In case of the pH dependent ^{113}Cd NMR measurements presented in Figure 4A, the peptide is loaded with 2 equiv of Cd(II) so that both sites are filled with metal. We have previously shown that the binding model for Cd(II) to these systems is that the metal first coordinates to the site of interest forming a $[Cd(pep)(Hpep)_2]^+$ species at low pH. As the pH is raised, two protons are released to give the tris thiolato complex $[Cd(pep)_3]^-$. Thus, the two relevant peptide species under low pH conditions are $[Cd(pep)(Hpep)_2]^+$ and $[Cd(pep)_3]^-$, while no apo peptide is present. Figure 4A shows that at low pH the 691 ppm peak dominates over the 681 ppm peak. With an increase in pH, the 681 ppm peak gains intensity over the 691 ppm peak and at pH 9.5 only the 681 (site B) and 686 (site A) ppm peaks are present. The 686 ppm peak gained intensity continuously during the course of the pH titration. The conversion from the 691 to the 681 ppm peak follows closely to the pK_{a2} determined for this peptide using UV−vis spectroscopy (Table 2).

One interpretation of the data in Figure 4A suggests that the 691 ppm peak may arise from site B (681 ppm) when Cd(II) in site B is present as $[Cd(pep)(Hpep)_2]^+$ and disappears when all the Cd(II) is present as only $[Cd(pep)_3]^-$ at site B. However, this model does not withstand the scrutiny of the data in Figure 4B. In this experiment, all spectra are collected at pH 9.5 which are conditions supporting only the $[Cd(pep)_3]^-$ metal structure. In the presence of only 1.0 equiv of Cd(II), we observe the simultaneous presence of both the peaks at 681 and 691 ppm. This observation suggests that the 691 ppm peak exists when the $[Cd(pep)(Hpep)_2]^+$ species at site B is absent. Therefore, considering the data in Figure 4A,B together, one can conclude that the 691 ppm peak cannot be an indicator of the presence of $[Cd(pep)(Hpep)_2]^+$ species at site B (681 ppm). Furthermore, the ^{113}Cd NMR resonance for $[Cd(pep)(Hpep)_2]^+$ has not been observed for a **TRI** peptide either as a dual site or mono site derivative,[3] and if observable, would be predicted to be far upfield of the $[Cd(pep)_3]^-$ chemical shift region. Thus, we eliminate a monothiolate Cd(II) species as the origin of the 691 resonance.

A second possible interpretation of these data is that the 691 ppm peak is an alternative form of the 686 ppm peak which is a consequence of the partial occupancy of site B that gives rise to the 681 ppm peak. Data in Figure 4B are consistent with this idea as it shows that in the presence of 1 equiv of ^{113}Cd(II) at pH 9.5 (where all the Cd(II) is present as $[Cd(pep)_3]^-$) indiscriminate binding is observed to both the Pen sites (681, 686, and 691 ppm). Subsequent changes upon addition of the second equivalent of the metal are also consistent with this interpretation. However, if we return to Figure 4A, which is collected under conditions where peptide is loaded with 2 equiv of ^{113}Cd(II) for all the spectra, we observe that the 691 peak appears at pH 7.5 through 8.2 even though site B (681 ppm) is

Table 5. Metalation States of the Two Pen Sites of **GRAND**L16PenL19IL23PenL26I and the Corresponding ^{113}Cd NMR Chemical Shifts under Different Experimental Conditions

Metalation state (site A)	Metalation state (site B)	^{113}Cd δ (ppm) (site A)	^{113}Cd δ (ppm) (site B)
$[Cd(pep)_3]^-$	apo	686	
$[Cd(pep)_3]^-$	$[Cd(pep)(Hpep)_2]^+$	686	ND^{a,b}
$[Cd(pep)_3]^-$	$[Cd(pep)_3]^-$	686	681
apo	$[Cd(pep)_3]^-$		691
$[Cd(pep)(Hpep)_2]^+$	$[Cd(pep)_3]^-$	ND^{a,b}	691

^{a} ND = not detected. ^{b} ^{113}Cd resonances for $[Cd(pep)(Hpep)_2]^+$or $[Cd(pep)(Hpep)_2(OH_2)]^+$ have never been detected for these or single site peptides such as Cd(II)(**TRI**L16C)$_3^-$.[32]

fully occupied with Cd(II). Therefore, we conclude that the 691 ppm peak cannot be an alternate form of the 686 ppm peak when site B is unoccupied because in these experiments (Figure 4A) site B is always filled.

Thus, we believe the model that best explains the data in both parts A and B of Figure 4 is that the 691 ppm peak is a form of the 681 ppm peak and exists when site A (686 ppm) is either unfilled (metal titration, apo) or present with only one deprotonated sulfur (pH titration, $[Cd(pep)(Hpep)_2]^+$). Furthermore, the 681 ppm feature only occurs when site A has a fully formed trigonal Cd(II) structure ($[Cd(pep)_3]^-$). Of course, the 681 and 686 ppm signals gain intensity as the pH is raised (Figure 4A) as a higher proportion of $[Cd(pep)_3]^-$ is formed in both the sites; however, the 681 specie dominates over the specie giving rise to the 691 ppm signal as all of the Cd(II) in site A becomes $[Cd(pep)_3]^-$ with increasing pH. Thus, the critical factor controlling the 10 ppm upfield shift of the ^{113}Cd NMR resonance is whether the final two thiolate sulfur atoms insert into the coordination sphere of the metal in site A. Hence, the 691 signal can appear either because an apo structure (present at high pH under substoichiometric conditions, Figure 4B) or a $[Cd(pep)(Hpep)_2]^+$ (present at lower pH under stoichiometric conditions, Figure 4A) structure occurring at site A (686 ppm). Recognizing this duality, it becomes clear that the switch between the 691 and 681 resonances is the rearrangement of the Pen side chains and subsequent structural/conformational change on going from an apo or partially bound $[Cd(pep)(Hpep)_2]^+$ form to the final $[Cd(pep)_3]^-$ structure. Such an explanation is consistent with X-ray structures of related systems that have recently appeared.[30,57,58] It can be concluded from the discussion of this section that the two sites in **GRAND**L16PenL19IL23PenL26I peptide are not completely independent of each other as Cd(II) bound to one of the sites (site B, 681 ppm) is perturbed by the metalation state (apo or $[Cd(pep)(Hpep)_2]^+$ or $[Cd(pep)_3]^-$) of the second center (site A, 686 ppm). Site A, on the other hand, seems to be insensitive to the metalation state of site B, based on the data presented in Figure 4, parts A and B. Of course one can hypothesize that site A is also being perturbed by the metalation state of site B and the resulting ^{113}Cd NMR signal(s) may be hidden under other peaks. However, based on the present data no definite conclusion can be drawn regarding this possibility. Table 5 summarizes these conclusions derived from Figure 4, parts A and B. Taking into consideration our previous designs of disubstituted peptides,[35,36,52] two layers of intervening Leu seem to be necessary to keep both metal centers completely inde-

(57) Peacock, A. F. A.; Stuckey, J. A.; Pecoraro, V. L. *Angew. Chem., Int. Ed.* **2009**, *48*, 7371–7374.

(58) Chakraborty, S.; Touw, D. S.; Peacock, A. F. A.; Stuckey, J. A.; Pecoraro, V. L. *J. Am. Chem. Soc.* **2010**, *132*, 13240–13250.

pendent. In the peptide **GRAND**L16PenL19IL23PenL26I there is only one intervening layer, Ile in this specific case, between both Cd(II) sites.

4.4. GRANDL12AL16CL26AL30C Peptide.

4.4.1. Physical Properties. With the **GRAND**L16PenL19-IL23PenL26I system well understood, we moved our attention to a peptide that should encapsulate two CdS_3O centers. The titration curve (Figure 1, blue color) following the binding of Cd(II) to **GRAND**L12AL16CL26AL30C is consistent with the complexation of 2($\pm$0.14) equiv of Cd(II) per trimer. The best description for the Cd(II) complex in this case is [Cd(II)-$(H_2O)]_2$(**GRAND**L12AL16CL26AL30C)$_3{}^{2-}$. This fully formed Cd(II) species has an extinction coefficient of 39 766 $M^{-1}cm^{-1}$ at 235 nm, which is lower than those of [Cd(II)]$_2$(**GRAND**-L16PenL19IL23PenL26I)$_3{}^{2-}$ (Figure 1, green color) and [Cd(II)]^{16}[Cd(II)(H$_2$O)]^{30}(**GRAND**L16PenL26AL30C)$_3{}^{2-}$ (Figure 1, red color) and, therefore, consistent with having two 4-coordinate sites.[34,36] To verify that both Cd(II) ions bind to the peptide **GRAND**L12AL16CL26AL30C as a 4-coordinate CdS_3O species, we carried out ^{111m}Cd PAC spectroscopic studies. The ^{111m}Cd PAC spectrum obtained under conditions that favored full loading of the peptide Cd(II), showed two different NQIs, namely NQI2 and NQI3, in addition to NQI4 that is present in almost all the spectra (Figure 6G). This result indicates the presence of different Cd(II) species on the ^{111m}Cd PAC time scale. The parameters for NQI2 ($\omega_0 = 0.342(6)$ rad/ns and $\eta = 0.148(8)$, Table 3) are very similar to those observed for **TRI**L12AL16C and has been assigned to a distorted tetrahedral CdS_3O species where the metal ion is most likely coordinated above the plane of the β-methylene protons of the Cys in an exo configuration, with an exogenous water molecule as a fourth ligand toward the N-terminus.[34,42] The lower frequency NQI3 signal ($\omega_0 = 0.242(8)$ rad/ns and $\eta = 0(1)$, Table 3) has parameters similar to those reported for the peptide **TRI**L16CL19A which presents a water-binding pocket below the metal binding site.[42] This peptide contains a 100% CdS_3O species and our best interpretation for this result is that Cd(II) is bound below the thiolate plane in an endo configuration with the water toward the C-terminus. This coordination geometry would resemble the one observed in the X-ray structure of As(**CSL9C**)$_3$,[30] (Coil-Ser (CS) is a crystallizable analogue of **TRI** family of peptides)[59] where As(III) is bound to the three Cys sulfurs below the plane defined by their β-methylene protons and the lone pair pointing toward the C-terminus. For Cd(II), the water molecule, as the fourth coordinating ligand, replaces the lone pair of electrons. The endo configuration could be favored for **TRI**L16CL19A because the generated hole lies just below the Cys. In contrast, the designed cavities for **GRAND**L12AL16CL26AL30C are located above the Cys sulfur plane; however, the Cys30 is located far toward the C-terminus of the peptide where helical fraying of the coiled coil is significant. This fraying should generate a more promiscuous binding center that would allow the water to enter from the C-terminal direction and coordinate to Cd(II). The NQI3 signal has never been observed for peptides containing the Cys at position 16 and which are capable of binding Cd(II) as a 100% CdS_3O species with an exo configuration (**TRI**L12AL16C, **TRI**L12AL16Pen, and **TRI**L9AL16C).[42] This observation suggests that in **GRAND**L12AL16CL26AL30C, NQI3 corresponds to the C-terminal binding site of L26AL30C. The corresponding

monosubstituted peptide, **GRAND**L26AL30C, showed essentially the same two NQIs (NQI2 and NQI3) (Figure 6B). Indeed, the amplitude corresponding to the NQI2 signal was smaller than that obtained for **GRAND**L12AL16CL26AL30C as would be expected since the peptide **GRAND**L26AL30C is missing the L12AL16C center (Table 3). Furthermore, the heterochromic peptide **GRAND**L16PenL26AL30C showed the same three NQI signatures which were observed under conditions where the peptide was in excess compared to Cd(II) (ratio peptide/Cd(II) = 12/1). This heterochromic peptide is known to bind Cd(II) in the L26AL30C center selectively both at low and high pH values (Figure 6C,D and Table 3).[36] This result supports the assignment that the L26AL30C center binds Cd(II) as a mixture of CdS_3O species, NQI2 and NQI3, best interpreted as to an exo and an endo configuration, respectively.

Once verified that the peptide **GRAND**L12AL16CL26AL30C binds 2($\pm$0.14) equiv of Cd(II) as 4-coordinate CdS_3O structures, we next investigated the pH dependence associated with this binding. The obtained pH titration curve (Figure 1, color blue) reveals that the second and third thiolates of this peptide bind to Cd(II) at lower pH values than those of the peptide **GRAND**L16PenL19IL23PenL26I. This observation is consistent with having 4-coordinate sites;[42] however, the pK_{a2} values obtained, 11.8 and 13.9, are not as similar to each other as those observed for Cd(II) binding to **GRAND**L16PenL19IL-23PenL26I (15.2 and 15.9). This is an interesting result since both sites are defined by the same type of residues and Cd(II) binds to both as CdS_3O species, as shown by ^{113}Cd NMR and ^{111m}Cd PAC spectroscopy. More importantly, these values are different from those obtained for the coordination of Cd(II) to the peptides **GRAND**L12AL16C ($pK_{a2} = 11.3$)[34] and **GRAND**L26AL30C ($pK_{a2} = 9.9$),[36,42] each containing only one binding site (Figure 2). Indeed, the simulated pH profile for 2 equiv of Cd(II) binding to **GRAND**L12AL16CL26AL30C with the pK_{a2} values of the individual sites (11.3 and 9.9) is quite different from the experimentally observed pH profile (Figure S7 of the SI). Upon closer examination of these data, one realizes that one of the pK_{a2} values (11.8) is close to the pK_{a2} value of Cd(II) binding to **GRAND**L12AL16C. Assigning the value of 11.8 to the pK_{a2} of Cd(II) binding to the site L12AL16C will imply that Cd(II) coordinates to the L26AL30C center with a pK_{a2} of 13.9. This represents a difference of 4 log units between having this binding site in **GRAND**L12AL16CL-26AL30C vs **GRAND**L26AL30C and **GRAND**L16PenL26-AL30C. The peptide **GRAND**L16PenL26AL30C is known to coordinate Cd(II) in the 4-coordinate site with a pK_{a2} of 9.6.[36]

4.4.2. Assignment of Individual pK_{a2} Values. At this point, it became essential to use NMR spectroscopy to assign the binding sites corresponding to these different pK_{a2} values. We first carried out ^{113}Cd NMR pH titrations. Two important observations can be inferred from the spectra shown in Figure 5. First, that the binding site with a ^{113}Cd chemical shift of 572 ppm binds Cd(II) at lower pH values than the site with a ^{113}Cd chemical shift of 589 ppm. Second, in contrast to **GRAND**L16PenL19IL23PenL26I (Figure 4A), the two binding centers in **GRAND**L12AL16CL26AL30C are independent of each other since additional ^{113}Cd chemical shifts were not observed for the half-loaded peptides. In this peptide, the two Cys sites are separated by two Leu layers (19 and 23), in addition to the Ala26 layer, and this can explain this different behavior. Comparing the resonances at 572 ppm and 589 ppm with those observed for the complexes [Cd(II)(H$_2$O)]-(**GRAND**L12AL16C)$_3{}^-$ (572 ppm)[42] and [Cd(II)(H$_2$O)]-

(59) Lovejoy, B.; Choe, S.; Cascio, D.; McRorie, D.; DeGrado, W.; Eisenberg, D. *Science* **1993**, *259*, 1288–1293.

(GRANDL26AL30C)$_3^-$ (588 ppm),[36] one is tempted to assign the Cd(II) binding pK_{a2} values of 11.9 and 13.8 to L12AL16C and L26AL30C sites of the peptide GRANDL12AL16-CL26AL30C, respectively.

To confirm these assignments, we directly monitored the ^{1}H chemical shifts of both Cys sites (Cys16 and Cys30) upon addition of Cd(II). Two-dimensional NOESY and TOCSY ^{1}H NMR spectroscopy were employed to assign the backbone resonances of the peptide (Figure S5). This information was used to identify the resonances of the β-methylene protons (H$^\beta$) of each Cys. Subsequently, ^{1}H–^{1}H NOESY experiments were carried out to monitor the binding of Cd(II) to Cys16 and Cys30 by observing the effects on resonances of the H$^\beta$ protons. If the assignments based on ^{113}Cd NMR spectroscopy are correct, the sequential additions of 0.5 equiv of ^{113}Cd(NO$_3$)$_2$ up to a total of 2 equiv at pH 6.0 should cause changes mainly in the region of the spectrum corresponding to the H^N-H$^\beta$ cross peak of Cys16. Figure 7 demonstrates that this indeed happens. A new major cross peak appears at 7.81 ppm (region **b**) that corresponds to the perturbation of the two individual H$^\beta$ resonances of Cys16 upon coordination of Cd(II) to this residue. These results indicate that at pH 6.0 Cd(II) binds primarily to Cys16 forming the species [Cd(II)(H$_2$O)]^{16}[apo]^{30}(GRANDL12A L16CL26AL30C)$_3^-$.

We further validated this assignment by carrying out a ^{113}Cd NMR spectrum of a solution containing 3.3 mM (GRAND-L12AL16CL26AL30C)$_3$ and 1.0 equiv of ^{113}Cd(NO$_3$)$_2$ at pH 6.0. This spectrum shows a single resonance at 572 ppm (Figure S3 of the SI) that corresponds to Cd(II) bound to the L12AL16C site. Next, we performed a pH-dependent NOESY experiment in the presence of 2 equiv of ^{113}Cd(NO$_3$)$_2$ (Figure S6 of the SI) and used this information for the assignment. The discussion related to the rest of the assignment section can be found in the SI. The combination of the UV–vis, ^{113}Cd NMR, and ^{1}H NMR spectroscopic data supports the conclusion that Cd(II) binds to the L12AL16C site with a pK_{a2} value of 11.8 and to the L26AL30C site with a pK_{a2} value of 13.9. In addition, these results have revealed a dynamic behavior of the L26AL30C site. The origin of this dynamic nature is not yet completely clear. However, the close proximity of this site to the edge of the α-helix, where fraying of the helices in the coiled coil is an important factor, could promote this situation. Indeed, ^{111m}Cd PAC spectroscopy shows how all the peptides containing the L26AL30C site display a mixture of NQI2, NQI3, and NQI4 (minor fraction), suggesting structural variability, whereas the L12AL16C only displays the NQI2. Despite this different behavior, the ^{113}Cd NMR spectrum (Figure S4) observed after addition of 1 equiv of ^{113}Cd(NO$_3$)$_2$ to a solution containing (GRANDL12AL16CL26AL30C)$_3$ at pH 8.5 shows Cd(II) coordination to both sites. Thus, Cd(II) does not show selectivity for either site at pH values where CdS$_3$O should fully exist in this peptide, as was observed for the CdS$_3$ centers in [Cd(II)]$_2$(GRANDL16PenL19IL23PenL26I)$_3^{2-}$.

4.4.3. Possible Reasons for the pK_{a2} Differences. The pK_{a2} value of [Cd(II)(H$_2$O)](GRANDL12AL16C)$_3^-$ is 11.3 and the L12AL16C site of [Cd(II)(H$_2$O)]$_2$(GRANDL12AL16CL26AL30C)$_3^{2-}$ is 11.8. The shift between these two values is relatively minor and requires little additional comment. However, the nearly 4 unit higher pK_{a2} of the L26AL30C site (13.9) in the GRANDL12AL16CL26AL30C peptide as compared to [Cd(II)(H$_2$O)](GRANDL26AL30C)$_3^-$ (9.9) deserves further consideration. GRAND peptides, by virtue of the additional heptad, are significantly more stable than the TRI peptides. Each substitution of Cys or Ala for Leu causes a marked disruption

of this stabilizing hydrophobic layer in either series. The GRAND peptides have 10 Leu layers (Table 1); however, in GRANDL12AL16CL26AL30C, four of these Leu layers have been modified causing as much as a 16–20 kcal/mol destabilization from the parent GRAND three stranded coiled coil.[27] Similarly, an 8–10 kcal/mol difference occurs between GRANDL12AL16CL26AL30C and a single site analogue (e.g., GRANDL12AL16C). Because the packing around the centrally located metal site L12AL16C should be only slightly destabilized by this overall decrease in free energy of association by adding the L26AL30C site, a small shift in pK_{a2} from 11.3 to 11.8 is reasonable. However, the L26AL30C is very close to the C-terminus, which already is expected to suffer from significant fraying.[30,57–59] The entire coiled coil is destabilized going from GRANDL26AL30C to GRANDL12AL16CL-26AL30C, especially by disrupting the center of the assembly. One might expect that this alteration could significantly perturb metal binding in the L26AL30C position, which is the inherently less stable site. One can envision that making a more stable aggregate by conferring improved packing at the C-terminus end of the GRANDL12AL16CL26AL30C peptide would shift the pK_{a2} values back toward more acidic range. To test this hypothesis, we designed the construct GRANDL12AL16-CL26AL30CL33I where Leu33 at the C-terminus end has been replaced by Ile which is known to render better packing. The resulting pK_{a2} values for this new construct are 11.6 and 13.5, respectively (Table 2, Figure 2 purple). The shift in pK_{a2} for the two sites of this new peptide is minor (0.2 and 0.4) from the parent GRANDL12AL16CL26AL30C peptide and is within the error of measurements. To understand the intricate interplay between peptide stabilities and the resulting pK_{a2} values, we analyzed the stability of the unmetalated GRAND-L12AL16C, GRANDL26AL30C, GRANDL12AL16CL-26AL30C, and GRANDL12AL16CL26AL30CL33I coiled coils using circular dichroism spectroscopy and guanidinium hydro-chloride (GuHCl) denaturation titrations (Figure S2 of the SI).

These experiments illustrate a significant decrease in stability of the GRANDL12AL16CL26AL30C construct as compared to the single site peptides GRANDL12AL16C and GRANDL26AL30C. Because of only a minor shift in the pK_{a2} value of GRANDL12AL16CL26AL30CL33I from GRAND-L12AL16CL26AL30C and due to the fact that the stability of the GRANDL12AL16CL26AL30CL33I construct could not be quantified, the relationship between pK_{a2} and aggregate stability could not be established. Understanding the intricate interplay between coiled coil stability and pK_{a2} would require future studies with many more protein constructs. However, we can qualitatively say that the explanation for the 4 unit shift in pK_{a2} between GRANDL26AL30C and GRANDL12AL16CL26-AL30C is, in part due to the general destabilization of the coiled coil by the addition of the second metal binding site at the middle of the peptide scaffold as it resulted in a significant destabilization of the coiled coil as observed by GuHCl denaturation studies. As a final note, preparing the dual CdS$_3$ construct GRANDL16PenL19IL23PenL26I from the parent GRANDL16Pen peptide is more tolerant to mutations because in this case, all of the residues replacing Leu (Pen or Ile) confer greater stability to the aggregate; however, one should recognize that to achieve such a dual 3-coordinate peptide still required the addition of a heptad (TRI to GRAND) and the incorporation of Ile for Leu.

5. Conclusions

In this work, we have investigated how the position of two metal binding sites that have "identical" first coordination environments within the three stranded α-helical coiled coils, can fine-tune the physical properties of bound metal ions [in this case, Cd(II)]. The peptide **GRAND**L16PenL19IL23-PenL26I, having a more rigid structure, binds two Cd(II) ions as trigonal planar 3-coordinate CdS$_3$ structures. Even though the physical properties of the two sites in this peptide are similar, these two sites are not completely independent of each other. The metalation state (apo or [Cd(pep)(Hpep)$_2$]$^+$ or [Cd(pep)$_3$]$^-$) of one site perturbed the Cd(II) bound to the second site. We found that a minimum of two Leu layers are required to keep both metal centers completely independent. The **GRAND**-L12AL16CL26AL30C peptide, that binds two Cd(II) ions as pseudotetrahedral 4-coordinate CdS$_3$O structures, shows a distinct behavior and displays different physical properties for the two metal sites. The pK_{a2} values, corresponding to the equilibrium [Cd(pep)(Hpep)$_2$]$^+$ $\rightarrow$ [Cd(pep)$_3$]$^-$ + 2H$^+$, range from 9.9 to 13.9, and the L26AL30C site shows dynamic behavior, which is not observed for the L12AL16C site. This is the combined effect of several factors playing a crucial role in determining the final properties of the bound Cd(II), among them, are the packing of the adjacent Leu residues, size of the intended cavity (endo vs exo) and location of the binding centers along the coiled coils. Thus, one can not define a location simply as a "4-coordinate" site without being cognizant of the numerous factors that determine the final physical properties of these types of structures.

It should be noted that there is not a 100% correspondence between the ^{113}Cd NMR shifts and the ^{111m}Cd PAC assessments of the CdS$_3$/CdS$_3$O ratio. Quantum chemical calculations show that a change in Cd$-$S bond length of 0.01 Å can cause a change in ^{113}Cd NMR chemical shift of $\sim$20 ppm (Hemmingsen et. al., unpublished results). Thus, the PAC data often indicate a higher percentage of CdS$_3$ in these samples than one would predict using the strict NMR correlation.

Supporting Information Available: Model and derivation of the pK_{a2} fitting equations for the dual site peptides, Table of the thermodynamic parameters determined from GuHCl-induced unfolding curves of peptides **GRAND**L26AL30C, **GRAND**-L12AL16C, and **GRAND**L12AL16CL26AL30C, GuHCl denaturation titration curves of **GRAND**L12AL16C, **GRAND**-L26AL30C, **GRAND**L12AL16CL26AL30C, and **GRAND**-L12AL16CL26AL30CL33I at pH 6.5, ^{113}Cd NMR of [Cd(II)(H$_2$O)]^{16}[apo]^{30}(**GRAND**L12AL16CL26AL30C)$_3^-$ at pH 6.0, ^{113}Cd NMR of (**GRAND**L12AL16CL26AL30C) with 1.0 equiv ^{113}Cd(II) at pH 8.5, NOESY spectrum of **GRAND**-L12AL16CL26AL30C showing sequential assignments of backbone amide protons, sections of NOESY spectra for **GRAND**-L12AL16CL26AL30C in the presence of 2.0 equiv of Cd(II) at different pH values, overlay of simulated and experimental UV$-$vis pH titration curves of **GRAND**L12AL16CL26AL30C, and part of the assignment. This material is available free of charge via the Internet at http://pubs.acs.org.

JA104433N